JOURNAL OF GUIDANCE, CONTROL, AND DYNAMICS
Vol. 16, No. 6, November–December 1993

Design and Piloted Simulation of Integrated Flight/Propulsion Controls for STOVL Aircraft

James A. Franklin* and Shawn A. Engelland†
NASA Ames Research Center, Moffett Field, California 94035

An integrated flight/propulsion control system has been designed for operation of short takeoff and vertical landing (STOVL) fighter aircraft over the low-speed, powered-lift flight envelope. The control system employs command modes for attitude, flightpath angle, and flightpath acceleration during transition, and translational velocity command for hover and vertical landing. In this paper, only the longitudinal modes of control are discussed. Piloted evaluations of the control system have been conducted on Ames Research Center's Vertical Motion Simulator. Results indicate that level 1 flying qualities are achieved during transition and vertical landing over a wide range of wind, atmospheric turbulence, and visibility conditions.

Nomenclature

AX_{CMD}	= axial acceleration command, ft/s^2
AZ_{CMD}	= normal acceleration command, ft/s^2
C_D	= drag coefficient
C_L	= lift coefficient
C_m	= pitching moment coefficient
$\bar{c}$	= mean aerodynamic chord, ft
d_e	= effective nozzle diameter, ft
g	= acceleration due to gravity, ft/s^2
$\dot{h}$	= vertical velocity, ft/s
I_{YY}	= pitch moment of inertia, slug-ft^2
K_{GE}	= ground effect washout factor
$\dot{m}$	= mass flow rate, slug/s
$\bar{q}$	= dynamic pressure, lb/ft^2
S	= wing area, ft^2
s	= Laplace operator
T, T_{TOT}	= total thrust, lb
u_B, w_B	= x and z axis velocity in body-axes system, ft/s
V, V_x	= longitudinal groundspeed, ft/s, kt
V_e	= jet velocity ratio; $\sqrt{\bar{q}/q_{\text{jet}}}$
W	= gross weight, lb
X, Z	= x and z axis moment arm, ft or axial and normal force, lbs
α	= angle of attack, deg
α_c	= commanded angle of attack; $\theta - \gamma_c$
γ	= flight path angle, deg
γ_c	= commanded flight path angle, deg
ΔD	= incremental drag due to direct thrust, lb
ΔL	= incremental lift due to direct thrust, lb
$\Delta L/T$	= jet-induced aerodynamic lift
$\Delta PM/T_{LN}d_e$	= jet-induced aerodynamic pitching moment
δ_E	= stabilator deflection, deg
δ_{LN}	= lift nozzle deflection (positive aft), deg
δ_{PCN}	= cruise nozzle pitch deflection (positive down), deg
δ_{PRCS}	= reaction control pitch thrust (down thrusting is positive), lb
θ	= pitch attitude angle, deg and rad
θ_N	= deflection of the total thrust component, deg
τ	= ratio of proportional to integral forward loop gain
IGE	= in ground effect
PLA	= power lever angle

Presented as Paper 91-3108 at the AIAA Aircraft Design Systems and Operations Meeting, Baltimore, MD, Sept. 23–25, 1991; received Nov. 18, 1991; revision received March 16, 1993; accepted for publication March 17, 1993.

*Aerospace Engineer. Associate Fellow AIAA.
†Aerospace Engineer. Member AIAA.

Introduction

INTEGRATION of flight and propulsion controls to achieve good flying qualities throughout the low-speed, powered-lift flight envelope is a critical technical issue for short takeoff and vertical landing (STOVL) aircraft. Poor flying qualities of the basic aircraft demand improvement for low-speed operation whereas the number and redundancy of aerodynamic and propulsion control effectors complicate the design of the control system for this flight regime. NASA is involved in the definition of control concepts, design methods and criteria, and the evaluation of these concepts in ground-based simulation of STOVL aircraft designs and in flight on the V/STOL Research Aircraft (VSRA). Attitude, flightpath, and flightpath acceleration command and stabilization systems (SCAS) for transition and translational velocity SCAS for hover and vertical landing have been designed for evaluation. The command modes and feedback control have been implemented in the form of a state-rate feedback implicit model follower to achieve the desired flying qualities and to suppress the effects of external disturbances and variations in the aircraft characteristics over the low-speed envelope.[1] A nonlinear inverse system was used to translate the ouput from these commands and feedback control into commands for the various aerodynamic and propulsion control effectors that are employed in powered-lift flight. The nonlinear inverse method has been applied previously in flight experiments on powered-lift short takeoff and landing (STOL) aircraft.[2,3] A moving-base simulation of a STOL configuration has been conducted to examine these control concepts over the low-speed flight envelope, including transition from conventional to vertical flight, hover, and vertical landing. This experiment was performed on the Vertical Motion Simulator at Ames Research Center. The evaluation included decelerating transitions to hover and vertical landing. Details of the complete control system design, cockpit displays, results of the simulation, control system performance, and design criteria are provided in Ref. 4. This paper only covers the design and evaluation of the longitudinal control modes for pitch attitude, longitudinal, and vertical velocity. Included are descriptions of the basic aircraft, its augmented flight controls, the simulation facility used in the experiment, the pilots' evaluation tasks and procedures, and the findings obtained from these experiments.

Description of the STOVL Aircraft Configuration

The STOVL aircraft investigated in this program is a single-place, single-engine fighter/attack aircraft with supersonic dash capability that was developed in the concept study phase of NASA's STOVL technology program. The aircraft, as shown in Fig. 1, features a blended wing-body configuration with a canted empennage. The wing is characterized by a leading-edge sweep of 50 deg and aspect ratio of 2.12. The propulsion system concept uses a turbofan engine in a mixed-flow remote lift arrangement, where the fan and core streams are either ducted forward to the lift nozzles (LN) or aft to a thrust deflecting cruise nozzle. A ventral nozzle (VN) can divert some of the aft flow to provide a pitching moment to counter that of the lift nozzles. Lift nozzle thrust can be deflected up to ± 20 deg about a nominal rearward cant angle of 8 deg. The cruise nozzle could be deflected laterally or vertically ± 20 deg. In conventional flight, the mixed flow is directed aft through the cruise nozzle, while in hover, it is diverted from the cruise nozzle to the forward lift nozzles, with a small portion reserved for the ventral nozzle. During transition from conventional to hover flight, the flow is smoothly transferred from the cruise to the lift nozzles.

The basic longitudinal flight-control system consists of a fully deflecting empennage for the aerodynamic effector during forward flight. Aerodynamic control during low-speed and hover flight is augmented by reaction control system (RCS) nozzles located in the tail powered by engine compressor bleed air, differential thrust transfer between the lift nozzles and ventral nozzle, and longitudinal deflection of lift nozzle thrust. Pitch control is achieved by a combination of symmetric empennage deflection, reaction controls, thrust transfer between the lift and ventral nozzles, and vertical deflection of the cruise nozzle. Longitudinal acceleration is achieved through thrust transfer between the lift and cruise nozzles and by deflection of the lift nozzle thrust.

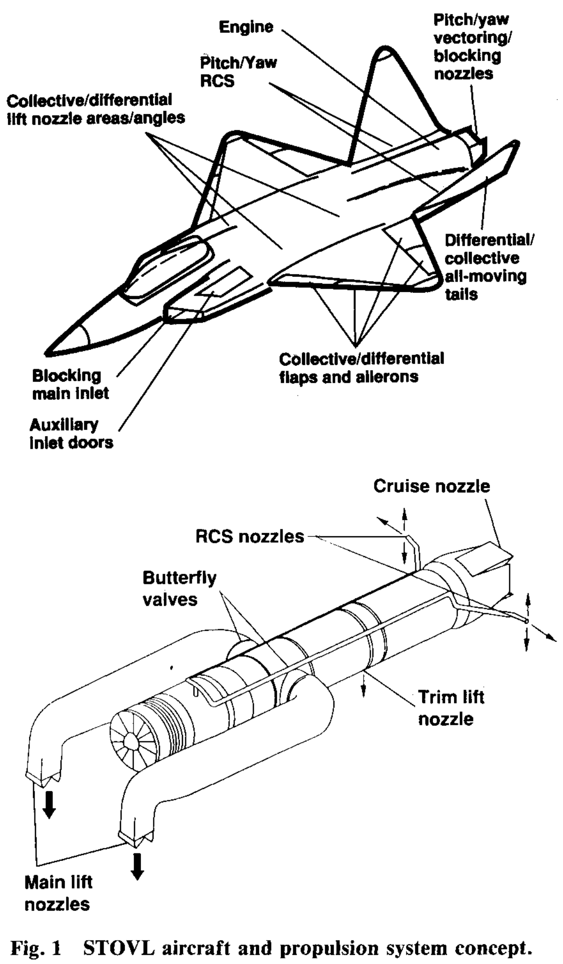

Fig. 1 STOVL aircraft and propulsion system concept.

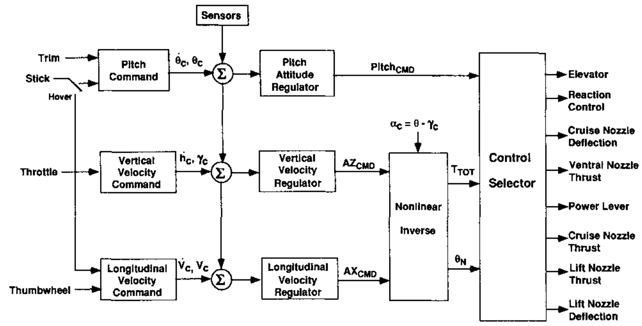

Fig. 2 Longitudinal SCAS block diagram.

To improve flying qualities of the basic aircraft, stabilization and command augmentation modes were provided. Based on experience in simulation of low-speed operations with V/STOL aircraft performing demanding instrument flight tasks,[1,5] a rate-command/attitude hold mode is employed during transition for pitch control, in conjunction with flightpath angle and flightpath acceleration command and hold modes. Pitch attitude command/attitude hold is used during hover with longitudinal and vertical translational velocity command. Although it will not be described in this paper, the lateral-directional SCAS included roll rate-command/attitude hold and yaw turn coordination in transition and roll attitude command/attitude hold and yaw rate command in hover.

A head-up display (HUD), that has been employed in several previous V/STOL simulations by NASA, provided the primary flight display for this simulation. The reader should consult Ref. 6 for a detailed description of its symbology and drive laws.

Integrated Flight/Propulsion Control System

An overview of the flight control system is shown in the block diagram of Fig. 2. The system is partitioned into the pilot's command inputs, the regulator that acts on the pilot's commands and sensed aircraft and propulsion system state variables, and the nonlinear inverse and control selector that couples these commands to the appropriate aerodynamic or propulsion control effectors. The pilot's commands and regulator are subdivided corresponding to pitch attitude control, and vertical and longitudinal translational velocity controls. Their command outputs are indicated on the diagram. The pilot's commands and regulator are defined by the flying qualities demanded by the mission task; minimal scheduling of command or feedback gains is necessary for variations in aircraft configuration and flight condition. The relationship of these gains to the desired dynamics typically is defined by linear, time-invariant, first- or second-order transfer functions. Variations in aircraft characteristics with changes in configuration and flight condition are incorporated in the nonlinear inverse. In the same vein, alterations in the aircraft's design, which changes the control system design, are accommodated by the nonlinear inverse as well. Each element of the system is covered in the following discussion.

Command Modes and Regulator

The pitch attitude control modes for transition and hover are a direct application of the state-rate feedback implicit-model following system that has been evaluated on a number of V/STOL aircraft simulations at Ames Research Center, including the AV-8 Harrier and the E-7A STOVL aircraft.[1,7] Its structure is shown in Fig. 3. The pilot's inputs are introduced through the control stick and trim switch. Either rate-command/attitude hold or attitude-command/attitude hold modes can be implemented, depending on whether the gain K_{111} is zero or not. The combination of angular acceleration feedback and proportional plus integral control produces a system that is insensitive to variations in aircraft configuration

Table 1 Attitude, flightpath, and velocity control mode dynamics

Control axis	Transition	Hover	Effector
Pitch	$\frac{\dot{\theta}}{\dot{\theta}_c} = \frac{4}{(s+2)^2}$	$\frac{\theta}{\theta_c} = \frac{4}{(s+2)^2}$	± 25 deg empennage thrust split 0-1250-lb RCS thrust ± 20 deg cruise nozzle
Vertical	$\frac{\gamma}{\gamma_c} = \frac{1}{s^2 + 1.4s + 1}$	$\frac{\dot{h}}{\dot{h}_c} = \frac{1}{s^2 + 1.4s + 1}$	3–100% power lever angle
Longitudinal	$\frac{V_x}{\dot{V}_{x_c}} = \frac{0.5(s+0.7)(s+2.86)}{s(s^2+1.8s+1)}$	$\frac{V_x}{V_{x_c}} = \frac{0.35(s+2.86)}{s^2+1.8s+1}$	0–102 deg θ_N

Table 2 Control mode gains

Pitch attitude control	Longitudinal velocity control	Vertical velocity control
Control limits = ± 5.65 in.	Control limits	$K_\gamma = 0.00545$ rad/deg
Force gradient = 1.0 lb/in.	Stick = ± 2.25 in.	$K_w = 0.71$ s^{-1}
Breakout = 0.15 in.	Thumbwheel = ± 100 deg	$K_{3W} = 0.14$
$K_{111} = 0.28$ rad/s/in.	Breakout	$\tau_{CNT} = 0.1$ s
$K_{222} = 0.31$ rad/in.	Stick = 0.225 in.	
$K_\theta = 4.0$ rad/rad	Thumbwheel = 5.5 deg	
$K_{\dot{\theta}} = 4.0$ s	$K_{2\dot{U}} = 0.1$	
$K_{300} = \frac{20.0}{1 + 0.0047\bar{q}}$ deg/rad	$K_{VI} = 20.0$ s^{-1}	
$\tau_9 = 0.05$ s	$K_V = 14.0$ ft/s^2/in.	
	$K_U = 0.69$ s^{-1}	
	$K_{3U} = 1.0$	
	$\tau_U = 0.35$ s	

and flight condition. Angular acceleration provides sufficient lead compensation to restore stability margins that are eroded by the integral control, while still maintaining the closed-loop gain to achieve the specified control bandwidth as well as good command tracking and disturbance rejection. Only the final forward loop gain (K_{300}) is changed in proportion to variations in sensitivity of the control effectors over the transition and hover envelope to maintain the desired dynamic response.

The flightpath and velocity control modes use a combination of the state-rate feedback concept along with the nonlinear-inverse system investigated in flight on the NASA Quiet Short Haul Research Aircraft and in simulation on the E-7A.[3,7] The state-rate feedback portion of the flightpath and velocity control is used to generate acceleration commands to the nonlinear-inverse system. For flightpath angle or vertical velocity command modes of Fig. 3, the throttle lever provides the pilot's command inputs. These, in combination with the vertical velocity and normal acceleration feedbacks, produce the acceleration command (AZ_{CMD}). Proportional plus integral control is employed in the forward loop. None of the gains are required to vary throughout transition or in hover to maintain the desired response. The velocity V_x is groundspeed along track and is used to convert the pilot's flightpath angle command to an equivalent vertical velocity command. For groundspeeds below 60 kt, this velocity is frozen at the 60 kt value to convert the pilot's command from flightpath angle to vertical velocity as is appropriate for hover and low-speed flight.

The longitudinal velocity control in Fig. 3 produces axial acceleration commands (AX_{CMD}) with a control structure similar to that for vertical velocity. During transition between forward flight and hover, the pilot commands longitudinal acceleration using a thumbwheel on the control stick. This mode is selected with switch E. Longitudinal acceleration and groundspeed combine with the pilot's commands and proportional plus integral feedforward to complete the control law. For precision hover, the thumbwheel is switched out and the control stick provides longitudinal velocity commands. In this mode, the stick is disconnected from the pitch attitude command system. While most of the hover maneuvering is performed at a constant pitch attitude, attitude changes can be made through the trim switch in Fig. 3.

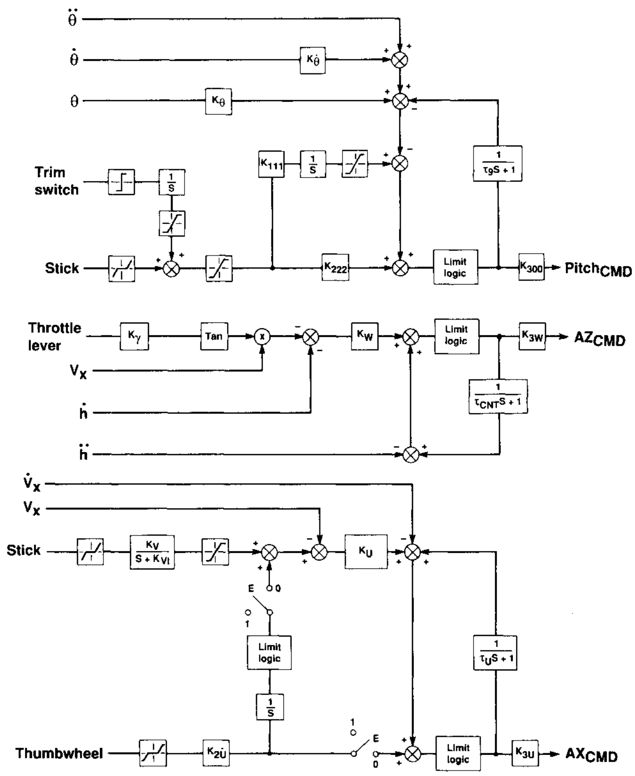

Fig. 3 Pitch attitude, vertical, and longitudinal velocity SCAS.

For each of these modes, integrator outputs are held when the control effectors for that axis reach their authority limits to prevent integrator windup.

Table 1 provides a description of the attitude, flightpath, and velocity command dynamic models. These models were chosen to provide level 1 flying qualities based on experience from similar applications to the NASA Harrier[1] as well as from industry programs and existing military flying qualities specifications for V/STOL aircraft. The associated control system gains that produce these model dynamics are listed in

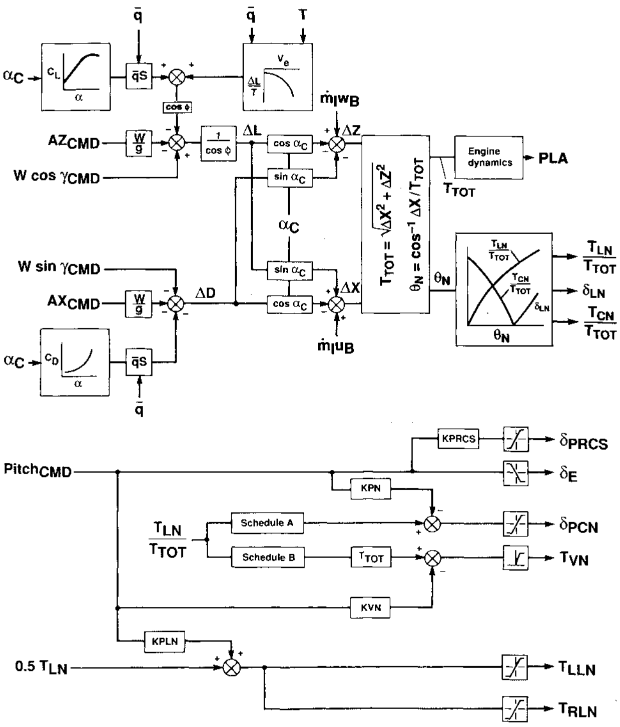

Fig. 4 Nonlinear inverse system and control selector.

Table 2. The gains are adapted, with only minor variations, from those applied to the Harrier.[1]

Nonlinear Inverse and Control Selector

The vertical and longitudinal acceleration commands from Fig. 3 are introduced to the nonlinear inverse portion of the system (Fig. 4), which solves the vertical and longitudinal force equations

$$mAZ_{\mathrm{CMD}} = Z + W\cos\gamma_c \quad \text{and} \quad mAX_{\mathrm{CMD}} = X - W\sin\gamma_c$$

to derive the thrust magnitude and deflection to satisfy these commands. The power-off and jet-induced aerodynamic contributions of the X and Z forces can be determined from current aircraft state measurements and knowledge of the aerodynamic characteristics as derived from powered-model wind tunnel tests and analytical predictions. They are shown in Fig. 4 as lift and drag curves and are implemented in the control system as multivariable table lookups. The increments in lift and drag that remain are resolved from flightpath into body axes and inlet momentum forces are extracted. The contribution to vertical and longitudinal forces that remain (ΔZ and ΔX) are those associated with thrust magnitude and thrust deflection, where thrust magnitude is simply the vector sum $T = \sqrt{\Delta X^2 + \Delta Z^2}$ and thrust deflection is $\theta_N = \cos^{-1}\Delta X\sqrt{\Delta X^2 + \Delta Z^2}$. The thrust magnitude and deflection of the individual nozzles required to produce the total thrust vector can then be determined by the control selector.

The control selector that converts pitch and thrust vector angle commands to commands for the individual aerodynamic and propulsion control effectors appears at the bottom of Fig. 4. Pitch commands are apportioned among the empennage, reaction control, lift nozzle and ventral nozzle thrust, and cruise nozzle deflection. Maneuvering inputs can be directed to each of the controls depending on the values of their respective gains. The empennage is considered to be the reference pitch control and is directly coupled to the pitch command. Gain K_{300} scales the pitch command in units of degrees of empennage deflection. The other pitch effectors' gains are scaled in relation to that for the empennage and are referenced per degree of empennage deflection. Thus KPRCS = 50 lb/deg and the pitch reaction control is limited to 1250 lbs thrust.

Table 3 Schedules for thrust split and lift nozzle deflection

θ_N, deg	$\dfrac{T_{\mathrm{LN}}}{T_{\mathrm{TOT}}}$	δ_{LN}, deg
0	0	20
10	0.17	20
20	0.30	20
30	0.43	20
40	0.55	20
50	0.67	20
64	0.82	20
74	0.84	10
83	0.86	0
92	0.88	−10
102	0.90	−20

The ventral nozzle gain KVN = $0.04(T_{\mathrm{VN}}/T_{\mathrm{TOT}})T_{\mathrm{TOT}}$ and the lift nozzle gain KPLN = $0.02(T_{\mathrm{VN}}/T_{\mathrm{TOT}})T_{\mathrm{TOT}}$ are scaled per degree of empennage and in addition by amount of thrust that is transferred to the ventral nozzle. Maximum ventral nozzle thrust is limited to 15% of total thrust (T_{TOT}) in the basic aircraft design.

Reaction control is used to provide high-bandwidth pitch control. Ventral nozzle thrust is used to supplement reaction controls for pitch maneuvering. Cruise nozzle deflection is used to augment the control power available from the other pitch effectors when necessary to maintain a desired level of pitch angular acceleration. Thus, the cruise nozzle gain is

$$\mathrm{KPN} = -0.04\sin^{-1}\left\{\frac{I_{YY}}{T_{\mathrm{CN}}X_{\mathrm{CN}}}\left[\ddot{\theta}_{\max} + \frac{25 - |\delta_E|}{I_{YY}}\left(K_{\mathrm{VN}}X_{\mathrm{VN}} + C_{m_{\delta_E}}\bar{q}S\bar{c} + K_{\mathrm{PRCS}}X_{\mathrm{RCS}}\right)\right]\right\}$$

The cruise nozzle pitch deflection and ventral nozzle thrust were also determined by the requirement to trim pitching moments from the lift nozzles and from jet-induced aerodynamics. These trim commands are generated by schedules A and B, respectively. The cruise nozzle schedule provides trim inputs up to ± 10 deg deflection with no ventral nozzle thrust commanded. When the pitch trim requirement exceeds that available from 10 deg of cruise nozzle, the nozzle is held at that position and ventral nozzle thrust is demanded to counter the remaining moment. The respective schedules are

Schedule A

$$|\delta_{\mathrm{PCN}}| < \pm 10\ \mathrm{deg} \qquad T_{\mathrm{VN}} = 0$$

$$\delta_{\mathrm{PCN}} = \sin^{-1}\left[\frac{1.02(1.057b - a)\dfrac{T_{\mathrm{LN}}}{T_{\mathrm{TOT}}} - \dfrac{\Delta M}{T_{\mathrm{TOT}}}}{X_{\mathrm{CN}}\left(1 - 1.079\dfrac{T_{\mathrm{LN}}}{T_{\mathrm{TOT}}}\right)}\right]$$

Schedule B

$$|\delta_{\mathrm{PCN}}| = \pm 10\ \mathrm{deg}$$

$$\frac{T_{\mathrm{VN}}}{T_{\mathrm{TOT}}} = \frac{a\dfrac{T_{\mathrm{LN}}}{T_{\mathrm{TOT}}} - 0.98b + \dfrac{\Delta M}{T_{\mathrm{TOT}}}}{c}$$

where

$$a = X_{\mathrm{LN}}\cos(\delta_{\mathrm{LN}} + 8) + Z_{\mathrm{LN}}\sin(\delta_{\mathrm{LN}} + 8) + 1.057b$$

$$b = -X_{\mathrm{CN}}\sin(10)$$

$$c = -0.99X_{\mathrm{VN}} - 0.139Z_{\mathrm{LN}} - 1.035b$$

$$\Delta M = [C_m(\alpha) + K_{\mathrm{GE}}\Delta C_{m_{\mathrm{IGE}}}]\bar{q}S\bar{c} + \left(\frac{\Delta PM}{T_{\mathrm{LN}}d_e}\right)T_{\mathrm{LN}}d_e$$

Thrust vector angle command determines the amount of thrust apportioned between the lift and cruise nozzles (thrust split) and the longitudinal deflection of these nozzles. The ratio of lift nozzle thrust to total thrust and lift nozzle deflection associated with this thrust split are presented in Table 3. Thrust magnitude is used to establish the total thrust command for the engine core.

Simulation Experiment

Simulator Facility

This experiment was conducted on the Vertical Motion Simulator at Ames Research Center. The simulator provides six-degree-of-freedom motion with large excursions in the vertical and longitudinal axes and large acceleration bandwidths in all axes that encompass the bandwidths of motion that are expected to be of primary importance to the pilot in vertical flight tasks. In the simulator cockpit, a three-window, computer-generated imaging (CGI) system provides the external view of an airfield scene representing the environs of Ames' experimental flight facility. An overhead optical combining glass projected the HUD for the pilot. A center stick and rudder pedal along with a left-hand throttle quadrant comprised the pilot's control inceptors. Computer frame time for the real-time digital simulation was 32 ms.

The aerodynamic and propulsion models from which this simulation was developed were derived from analytical predictions and small-scale wind tunnel tests of the aircraft and from an analytical model of the propulsion system. Aerodynamic characteristics included jet-induced effects from propulsion system flows both in and out of ground effect in addition to power-off characteristics in wingborne flight. Propulsion system characteristics include gross thrust maps as a function of fan speed, ambient temperature, and compressor bleed flow. Rate-limited, second-order dynamic response of gross thrust, dynamic response of flow through ducts to the remote components, and duct flow and nozzle efficiency factors were represented in the model.

Evaluation Tasks and Procedures

The pilot's operational tasks for evaluation during the simulation were curved decelerating approaches to hover, followed by a vertical landing on the airfield. The approach was initiated under instrument meteorological conditions (IMC) in level flight at 1100-ft altitude at 200 kt in the landing configuration. The aircraft's initial position was offset from the final approach course on a relative intercept heading of 65 deg. The sequence of events for the initial phase was a 3-deg glideslope capture, commencement of a 0.1-g nominal deceleration, a turn to align with the final approach course, and, on short final at a range of 1000 ft, a change in nominal deceleration rate to 0.05 g. Desired performance was defined as keeping glideslope and localizer excursions within 0.75 deg. Adequate performance was achieved when tracking excursions were significant, but not divergent. Meteorological conditions consisted of a ceiling of 100 ft and a visual range of 1200 ft in fog with wind varying up to a maximum of 34 kt at 30 deg to the left of the final approach course and with an rms turbulence up to 6 ft/s. Acquisition of the hover 43 ft above the landing surface completed the approach.

The vertical landing was accomplished on a 100×200-ft landing pad on the runway. Desired landing performance was defined as touchdown within a 5-ft radius of the center of the pad with a sink rate of 3–5 ft/s. Adequate performance was considered to be touchdown within the confines of the pad at sink rates less than 12 ft/s and with minimal lateral drift. Wind conditions for the runway landings were identical to those for the approach.

Three pilots with V/STOL and powered-lift aircraft experience performed as evaluation pilots in this experiment. Pilot ratings and comments were obtained, based on the Cooper-Harper scale.[8]

Discussion of Results

IMC Decelerating Transition

The pilots' evaluations of the transition are shown in Fig. 5. The effect of turbulence up to an rms level of 6 ft/s is indi-

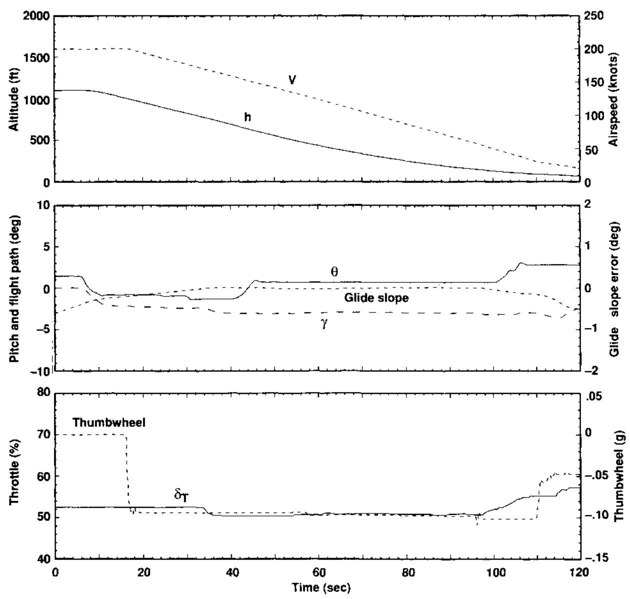

Fig. 6 Time history of IMC decelerating transition.

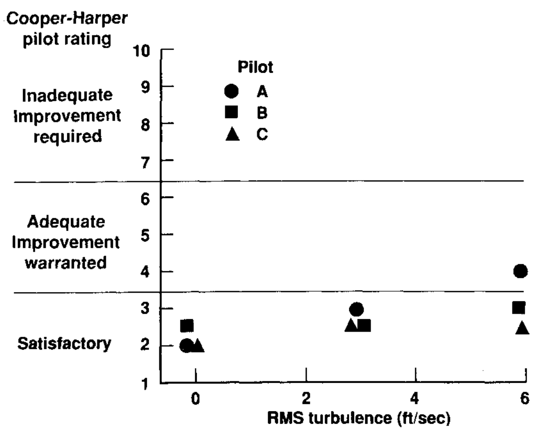

Fig. 5 Pilot evaluations of flying qualities for IMC decelerating transition.

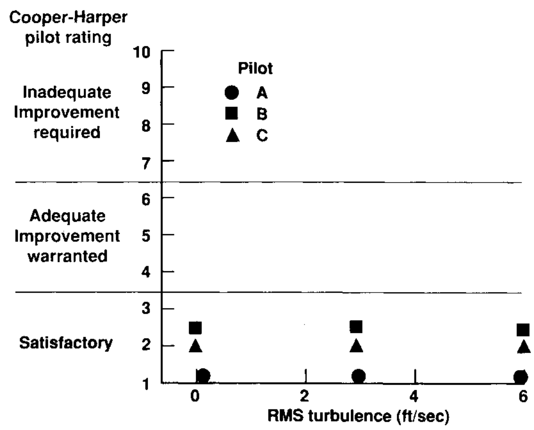

Fig. 7 Pilot evaluations of flying qualities for vertical landing.

cated. The flightpath SCAS yielded satisfactory flying qualities over the range of wind and turbulence conditions, with only slight degradation at the highest level of turbulence. This control mode only required a minimum of effort by the pilot for the overall approach task, most of which was associated with making small adjustments to counteract the effects of turbulence during the early stages of the approach when the aircraft was in substantially wing-borne flight. In all cases, desired performance was achieved with the flightpath SCAS.

A representative time history of the decelerating transition to the decision height of 100 ft is presented in Fig. 6 for the flightpath SCAS system in calm air. Pitch attitude is initially used for flightpath control and then is fixed as the pilot completes the approach using the throttle for flightpath control. Glideslope capture and tracking is smooth and precise. Deceleration commands are introduced in a few discrete steps through the thumbwheel. At the final stage of the approach, the deceleration rate is reduced in preparation for acquiring the hover point.

Vertical Landing

Pilot evaluations for vertical landings on the runway are shown in Fig. 7. These ratings apply to the hover position control and vertical descent to touchdown following the decelerating transition and acquisition of the hover point. Results are presented for three levels of turbulence. The translational velocity SCAS was judged to be fully satisfactory by all pilots regardless of the level of turbulence. The system allows the pilot to quickly and precisely set the desired sink rate and maintain that to touchdown. The control system was effective in suppressing the effects of wind and turbulence, in part because the aircraft's aerodynamic response to turbulence is substantially less in hover than for the transition.

Conclusions

An integrated flight/propulsion control system was developed for a STOVL aircraft concept and was evaluated throughout the low-speed flight envelope. The control system provided command modes for attitude, flightpath angle and flightpath acceleration during transition, and translational velocity command for hover and vertical landing. Only the longitudinal modes are discussed in this paper. The command modes and feedback control were implemented in the form of a state-rate feedback implicit model follower to achieve the desired flying qualities and to suppress the effects of external disturbances and variations in the aircraft characteristics over the low-speed envelope. The system employed proportional-plus-integral control along with acceleration feedback to achieve good stability margins and to suppress effects of variation in configuration and flight condition. A nonlinear inverse system was used to translate the output from these commands and feedback control into commands for the various aerodynamic and propulsion control effectors that are employed in powered-lift flight. To achieve the dynamic response desired for good flying qualities, it was only necessary to vary the pitch forward loop gain; all other gains were held constant.

Evaluations were conducted during decelerating transitions under instrument flight conditions followed by airfield landings to evaluate the flying qualities for the integrated control modes. Pilots' assessments indicated that level 1 flying qualities could be achieved for deceleration to hover in instrument conditions and for airfield landings when attitude and velocity stabilization and command augmentation control modes were provided. Results were largely insensitive to levels of wind and turbulence.

References

[1]Moralez, E., Merrick, V. K., and Schroeder, J. A., "Simulation Evaluation of an Advanced Control Concept for a V/STOL Aircraft," *Journal of Guidance, Control, and Dynamics,* Vol. 12, No. 3, 1989, pp. 334–341.

[2]Meyer, G., and Cicolani, L., "Application of Nonlinear Systems Inverses to Automatic Flight Control Design-System Concepts and Flight Evaluations," AGARDograph No. 251, July 1981.

[3]Franklin, J. A., Hynes, C. S., Hardy, G. H., Martin, J. L., and Innis, R. C., "Flight Evaluation of Augmented Controls for Approach and Landing of Powered-Lift Aircraft," *Journal of Guidance, Control, and Dynamics,* Vol. 9, No. 5, 1986, pp. 555–565.

[4]Franklin, J. A., Stortz, M. W., Engelland, S. A., Hardy, G. H., and Martin, J. L., "Moving Base Simulation Evaluation of Control System Concepts and Design Criteria for STOVL Aircraft," NASA TM 103843, June 1991.

[5]Lebacqz, J. V., Merrick, V. K., and Franklin, J. A., "Control and Display Requirements for Decelerating Approach and Landing of Fixed- and Rotary-Wing V/STOL Aircraft," American Helicopter Society Paper A-86-42-70-100, 1986.

[6]Merrick, V. K., Ferris, G. G., and Vanags, A. A., "A Head-Up Display Format for Application to V/STOL Approach and Landing," NASA TM 102216, Jan. 1990.

[7]Franklin, J. A., Stortz, M. W., Gerdes, R. M., Hardy, G. H., Martin, J. L., and Engelland, S. A., "Simulation Evaluation of Transition and Hover Flying Qualities of the E-7A STOVL Aircraft," NASA TM 101015, Aug. 1988.

[8]Cooper, G. E., and Harper, R. P., Jr., "The Use of Pilot Rating in the Evaluation of Aircraft Handling Qualities," NASA TN D-5153, April 1969.